

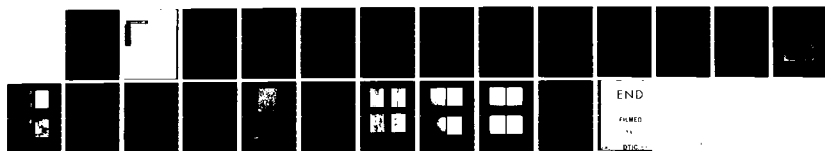
HD-A131 759

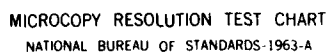
APPLICATION OF RAPIDLY SOLIDIFIED SUPERALLOYS(U) PRATT 1/1  
AND WHITNEY AIRCRAFT GROUP WEST PALM BEACH FL A R COX  
NOV 77 PWA-FR-9417 F33615-76-C-5136

UNCLASSIFIED


F/G 11/6

NL





MICROCOPY RESOLUTION TEST CHART  
NATIONAL BUREAU OF STANDARDS-1963-A



UNCLASSIFIED

SECURITY CLASSIFICATION OF THIS PAGE (When Data Entered)

REPORT DOCUMENTATION PAGE		READ INSTRUCTIONS BEFORE COMPLETING FORM
1. REPORT NUMBER	2. GOVT ACCESSION NO. AD-A131759	3. RECIPIENT'S CATALOG NUMBER
4. TITLE (and Subtitle) APPLICATION OF RAPIDLY SOLIDIFIED SUPERALLOYS		5. TYPE OF REPORT & PERIOD COVERED Quarterly Report 1 August 1977 — 31 October 1977
		6. PERFORMING ORG. REPORT NUMBER FR-9417
7. AUTHOR(s) A. R. Cox		8. CONTRACT OR GRANT NUMBER(s) F33615-76-C-5136
9. PERFORMING ORGANIZATION NAME AND ADDRESS United Technologies Corporation Pratt & Whitney Aircraft Group Government Products Division Box 2691, West Palm Beach, Florida 33402		10. PROGRAM ELEMENT, PROJECT, TASK AREA & WORK UNIT NUMBERS
11. CONTROLLING OFFICE NAME AND ADDRESS Defense Advanced Research Projects Agency 1100 Wilson Boulevard Arlington, Virginia 22209 (Dr. E. C. vanReuth)		12. REPORT DATE November 1977
		13. NUMBER OF PAGES 20
14. MONITORING AGENCY NAME & ADDRESS (if different from Controlling Office) Air Force Materials Laboratories Wright-Patterson Air Force Base, Ohio 45433 (Mr. A. Adair)		15. SECURITY CLASS. (of this report) Unclassified
		15a. DECLASSIFICATION DOWNGRADING SCHEDULE
16. DISTRIBUTION STATEMENT (of this Report) Approved for Public Release, Distribution Unlimited		
17. DISTRIBUTION STATEMENT (of the abstract entered in Block 20, if different from Report)		
18. SUPPLEMENTARY NOTES		
19. KEY WORDS (Continue on reverse side if necessary and identify by block number) Superalloys, Powder Metallurgy, Rapid Solidification, Turbine Airfoils, Centrifugal Atomization, Convective Cooling		
20. ABSTRACT (Continue on reverse side if necessary and identify by block number) This program is being conducted for the purpose of applying the principle of rapid solidification to superalloy powders and subsequent development of a stronger alloy composition for jet engine turbine airfoils. Centrifugal atomization and forced convective cooling are being used to produce the fast-cooled material.  During this report period, heat treat studies to produce aligned grain structures, thermal stability evaluation, and initial mechanical property tests were run for 4 classes of experimental alloys. Results showed that 3 classes of alloys heat treated effectively and one of the alloys achieved levels of creep rupture strength commensurate with program goals.		

DD FORM 1 JAN 73 1473

EDITION OF 1 NOV 65 IS OBSOLETE

S N 0102-LF-014-6601

UNCLASSIFIED

SECURITY CLASSIFICATION OF THIS PAGE (When Data Entered)

## CONTENTS

Section	Page
I INTRODUCTION.....	2
II MATERIALS EVALUATION.....	3
Initial Alloy Screening.....	3
Extrusion.....	3
Testing With Equiaxed Grain Microstructures.....	4
Aligned Grain Microstructures.....	5
Thermal Stability.....	7
Test Results With Aligned Grain Structures.....	9
III ON-GOING STUDY.....	17

Application For	
DTIC GRAAL	<input checked="" type="checkbox"/>
DTIC F&B	<input type="checkbox"/>
Unannounced	<input type="checkbox"/>
Justification	
By _____	
Distribution/	
Availability Codes	
Dist	Avail and/or Special



## ILLUSTRATIONS

<i>Figure</i>		<i>Page</i>
1	Thermal Stability of RSR 121 After 300 hr at 1600°F (871°C).....	7
2	Thermal Stability of RSR 104 After 300 hr at 1600°F (871°C).....	8
3	Thermal Stability of RSR 116 After 300 hr at 1600°F (871°C).....	8
4	Transmission Photomicrograph Showing the Structure of RSR 104 After Zone Annealing.....	12
5	Typical Creep Deformation of Experimental Alloys at 1900°F (1038°C) and 14.2 ksi (97.9 MPa).....	12
6	Creep Resistance of Experimental Alloys (Time to 1% Elongation).....	13
7	Stress-Rupture Life of Experimental Superalloys.....	13
8	Typical Failure Characteristics of Experimental Superalloys.....	14
9	Microstructure of RSR 121 After Creep-Rupture Testing at 1800°F (982°C) and 30.5 ksi (210.3 MPa), Failure Time = 44 hr.....	15
10	Microstructure of RSR 121 After Creep-Rupture Testing at 1900°F (1038°C) and 14.4 ksi (99.3 MPa), Failure Time = 219 hr.....	15
11	Microstructure of RSR 116 After Creep-Rupture Testing at 1900°F (1038°C) and 14.4 ksi (99.3 MPa), Failure Time = 149 hr.....	16
12	Microstructure of RSR 104 After Creep-Rupture Testing at 1900°F (1038°C) and 30 ksi (206.8 MPa), Failure Time = 34 hr.....	16

## TABLES

<i>Table</i>		<i>Page</i>
1	Superalloy Compositions.....	4
2	Alloys Responding to Heat Treatment for Aligned Grain Structures.....	5
3	Solutioning Temperatures Used to Heat Treat Experimental Alloys.....	9
4	Creep-Rupture Results of RSR Alloys Having Aligned Grain Structures.....	10
5	Activation Energy For Matrix Creep in MAR M200 Alloy.....	11

## **SUMMARY**

This program is being conducted for the purpose of applying the principle of rapid solidification to superalloy powders and subsequent development of a stronger alloy composition for jet engine turbine airfoils. Centrifugal atomization and forced convective cooling are being used to produce the fast-cooled material.

During this report period, heat treat studies to produce aligned grain structures, thermal stability evaluation, and initial mechanical property tests were run for 4 classes of experimental alloys. Results showed that 3 classes of alloys heat treated effectively, and one of the alloys achieved levels of creep rupture strength commensurate with program goals.



## SECTION I

### INTRODUCTION

The performance improvements of current military gas turbines, such as the Pratt & Whitney Aircraft F100, over earlier engines were made possible through advancements in design technology and materials processing. Better alloys, by virtue of chemical composition, played only a minor role in achieving present day capability. Future engine projections, however, demand that better materials be developed in order that still higher levels of performance can be achieved.

The turbine module is especially dependent on improvements in such alloy properties as high temperature capability, better stability, and better corrosion resistance. The alloys presently being used in the turbine module were developed more than 15 years ago. These alloys are still in use, not because of a lack of interest in development but rather, due to the inability to improve the nature of alloying under conditions now imposed for subsequent processing and component fabrication. Precision casting alloy compositions are limited because of such constraints as crucible and mold interactions and massive phase occurrence. Forging alloys are limited because of constraints of segregation during ingot processing.

Superalloy powder metallurgy studies conducted at the P&WA/Florida facility have shown that the use of powder, particularly powder solidified at very high rates of cooling, can eliminate the constraints noted and can enable more effective alloying for the improvement of basic material properties. Several examples which support this statement are as follows. Chemical segregation in fast cooled superalloy powders can be controlled to a submicron level. Massive phases can be eliminated. Solubility of alloying elements can be extended without deleterious phase reaction. None of these can be achieved in ingot or precision casting.

Further, the inherent homogeneity of the powder is such that subsequent processing and heat treatment can be used very effectively to promote maximum material utilization. Abnormal grain growth, for example, can be achieved in superalloy powder materials for optimization of mechanical properties above  $\frac{1}{2} T_m$ . MAR M200 alloy powder, processed and reacted in this manner, is, in fact, stronger than, and as ductile as, the same composition cast in a directional mode.

P&WA/Florida has constructed a device that can produce metal powders solidified and cooled at rates in excess of  $10^6$  °C/sec. The underlying principle is forced convective cooling, whereby liquid particles of controlled size are accelerated into a high thermal conductivity gaseous medium maintained at high  $\Delta T$  between itself and the particles.

The purpose of this Advanced Research Projects Agency (ARPA) sponsored program is to refine the process mechanics used with the powder producing device for fast quenching bulk lots of powder and, subsequently, applying the technology of rapid solidification to the development of an alloy composition that is stronger than the existing MAR M200 alloy and that can be implemented for the production of better turbine airfoils.

The program is a 40-month effort and is organized as a progression of events starting with a parametric study of the requirements necessary to achieve high yields of fast quenched powder and terminating in the fabrication and testing of turbine airfoils. This is the seventh technical report and covers the 19th through 21st months of the program. It deals with the evaluation of experimental alloys, produced as fast cooled powders.

## SECTION II

### MATERIALS EVALUATION

#### INITIAL ALLOY SCREENING

In the previous two technical reports, we cited work accomplished with some 40 experimental compositions relative to consolidation, working, and alloy microstructural change caused by various thermal exposures. This report describes the completion of effort with these compositions, as a group, and includes the results of mechanical property testing as well as additional studies of alloy stability.

These alloys have been reported previously and were selected to determine superalloy types or classes which would respond most favorably to the effects of rapid solidification. Basically, this selection covered four categories of superalloys, as listed below:

1. Typical nickel base superalloys, comprised of varying quantities of  $\gamma'$  and solid solution strengtheners, and with varying types of dispersions (based on interstitial addition).
2. Compositions normally referred to as Directionally Solidified (DS) Eutectics.
3. Compositions based on the ternary Ni-Al-Mo system.
4. Simple high volume fraction  $\gamma'$  alloys with varying refractory and interstitial additions.

For the most part, these compositions can be traced to alloys which have been studied by numerous investigators and which have been published in the open literature.

This original group of alloys was reduced to 23 for study during this period, and, along with our category designations, are listed in Table 1. The compositions which were eliminated were those which represented only minor departures from alloys included in this on-going study and which, in our opinion from earlier work, would not compromise the intent of effort.

#### EXTRUSION

All 23 of these alloys were extruded at AFML during the previous report period and the basic results were reported in the August 1977 report. Some additional extrusions were made during this time to provide more bar stock for study and, generally, the results were no different from those described earlier. It was noted, however, that the conventional type superalloys (as evidenced in MAR M200, AF2-1DA and MAR M247 alloys, the latter being processed as an adjunct to this program) exhibited some centerline cracking when processed above the secondary phase  $\gamma'$  solvus. This was attributed to hot shortness. Beyond this, it was our judgment that the bar stock showed no anomalies. Oxygen levels were typically 75 ppm or less, and such possible degradations as particle surface reactions or variances in alloy macro/microstructure along the length of the bar were not detected. Contamination concentrations of a type attributable to our master heat or powder processing methods were determined to be on the order of 3 ppm and were considered totally satisfactory for our work.

TABLE 1. SUPERALLOY COMPOSITIONS

ID	Element (Wt %)													Category
	Ni	Co	Cr	Al	Ti	C	B	Mo	Zr	Ta	W	Nb	Other	
87	Bal	10.0	8.8	5.2	1.4	0.14	0.018	3.2	0.12	5.3	6.2			1
90	Bal	10.2	10.8	4.2	3.3	0.58	0.018	3.3	0.13	3.1	6.4			1
96	Bal		10.0	6.0	1.0	0.01	0.01		0.02	8.0	6.0			1
108	Bal	10.0	9.0	5.0	2.1	0.15	0.015				12.5	1.0		1
121	Bal	10.1	10.6	4.2	3.2	0.29	0.018	3.3	0.12	3.1	6.3			1
122	Bal	10.1	10.7	4.2	3.3	0.29	0.055	3.3	0.12	3.1	6.3			1
124	Bal	10.0	9.0	5.0	2.0	0.01	0.10		0.05		12.5	1.1		1
97	Bal	10.0	10.0	5.0		0.5					10.0	4.7		2
99	Bal	20.0	10.0	4.0		0.6					10.0	4.9		2
100	Bal			9.0				27.2						2
101	Bal			6.2				31.5						2
102	Bal			4.7				34.6						2
103	Bal			8.4				15.0						3
104	Bal			8.0				18.0						3
105	Bal			7.6				21.0						3
123	Bal			9.2				11.5						3
110	Bal		9.3	8.5	1.1	0.21					6.6			4
111	Bal		9.6	8.7		0.17							3.25 Hf	4
112	Bal		9.8	8.9	1.1	0.21								4
113	Bal		9.7	7.7	2.0	0.21						1.7		4
116	Bal		9.1	8.3		0.05					9.5			4
117	Bal		9.9	8.3		0.20					9.3			4
119	Bal		9.7	7.7	0.9	0.19						3.0		4

\*Based on master heat charge weight

- Category
- 1 - Conventional Superalloy Type
  - 2 - DS Eutectic Type
  - 3 - Ni-Al-Mo Ternaries
  - 4 - High  $\gamma$  Type

### TESTING WITH EQUIAXED GRAIN MICROSTRUCTURES

The original purpose with these alloys was to study how the individual compositions responded to heat treatment, and how they would react under conditions of long time thermal exposure. Those alloys which underwent degenerate reactions, or suggested instability by way of easy phase coalescence, could thus be eliminated, thereby providing a simple screening process whereby only the most heat-resistant alloys would remain for continued evaluation.

Although it was an accepted fact that an elongated grain structure would be a requisite for alloy implementation into turbine airfoils, we elected to compliment these thermal studies with mechanical property tests based on equiaxed test bars. This approach appeared to be an expedient means of adding to our knowledge of how a particular alloy behaved, without the need to exploit unidirectional grain growth at that time, and when combined with the microstructural evaluation, would conceivably provide total validity to the screening process. Additionally, it was felt that judicious selection of creep-rupture parameters in the 1800 to 1900°F (982 to 1038°C) range, and rigid treatment of the resulting data, could lead to a determination of activation energy for matrix creep which, in turn, could be used as a quantified index of potential alloy value.

All 4 alloy categories were subjected to this test procedure. The particular alloys used were RSR 87, 97, 103, 108, 111, 113, 117, and 119. Each alloy was given a 4-hour anneal at the predetermined temperature for maximum grain coarsening as discussed in the August 1977 report. Subsequently, the alloys were exposed to a 1975°F (1079°C) cycle for 4 hours (coating simulation) and 1600°F (871°C) cycle for 12 hours (typical age).

Testing was started at 1900°F (1038°C) and 15,000 psi (103.4 MPa), corrected to the density of MAR M200. The stress level was picked so that further testing at the same stress could be effectively carried out at higher temperatures. Unfortunately, the data we generated was sporadic and typically short in time to failure (1.5, 15.1, 28 hr, etc.). Determination of second stage creep rates was difficult and elimination of the grain boundary contributions from total creep was done with questionable precision. Further, our calculations gave activation energies for matrix creep which varied more than 50% in some instances (75kcal - 215kcal/m for example), depending on alloy and which set of test data were used. Therefore, we felt that continued work along these lines would not improve upon our ability to understand the basic set of compositions, and that values such as these were indicative of macro conditions associated with the test bars rather than with the specific compositions. Accordingly, after some 30 test starts, we discontinued the approach.

### ALIGNED GRAIN MICROSTRUCTURES

With the discontinuation of equiaxed test bar evaluations, efforts to produce aligned grain structures in bar stock quantities sufficient for mechanical testing were stepped up. Previously, we had found that within the process constraints imposed, 8 of the 23 alloys showed a propensity toward abnormal grain growth and subsequent grain alignment. From additional work during this period, we found that a total of 16 of the 23 could be heat treated to aligned grain structures and, of these, 14 could be controlled well enough to produce barstock for testing.

These studies were carried out in a zone annealing furnace capable of controlling to about  $\pm 25^\circ\text{F}$  ( $\pm 14^\circ\text{C}$ ), operating the annealing zone at the temperature where most pronounced grain growth was observed from prior gradient bar evaluation and under a temperature gradient of about 100 to 150°F/in. (22 to 33°C/cm). Traversing times for test bar heat treating were on the order of 0.4 to 0.5 in. (1.0 to 1.3 cm) per hour.

The alloys which showed a response to aligned grain structure heat treating are listed in Table 2. Alloys 87 and 96 were the 2 alloys which did not respond well enough for processing into test bar stock. The following paragraphs describe the overall results of zone heat treating with respect to our defined alloy categories.

TABLE 2. ALLOYS RESPONDING TO HEAT TREATMENT FOR ALIGNED GRAIN STRUCTURES

---

RSR 87
RSR 96
RSR 103
RSR 104
RSR 105
RSR 108 <sup>1</sup>
RSR 110
RSR 112
RSR 113
RSR 116
RSR 117
RSR 119
RSR 121
RSR 122
RSR 123
RSR 124

---

<sup>1</sup> Also, RSR 57, 58, 60, and 61 which are other runs of MAR M200 alloy, the details of which are listed in the February 1977 report

### **Conventional Superalloys (RSR 87, 90, 96, 108, 121, 122, 124)**

Of this group, only RSR 90 failed to respond at all to aligned grain processing. This alloy showed no tendency toward grain coarsening in earlier gradient bar studies and was attributed to a relatively large volume fraction of carbide present in the alloy microstructure (0.58% C). The carbide phase was somewhat coarse (typically 1 to 5  $\mu\text{m}$ ) and stable up to the incipient melt point.

Limited success was achieved with RSR 87 and 96. For RSR 87, the response was one in which abnormal grain growth took place in the peripheral regions of the bar stock, leaving coarse, equiaxed grains in the center. This condition has been observed by others as a result of the processing parameters. We will attempt to do more of this work as deemed necessary by results of subsequent testing.

For alloy 96, the gamma prime dissolution temperature was essentially the same as the incipient melt temperature, and it was difficult to determine furnace operating parameters which would not cause partial destruction of the bar through localized melting. The alloy showed numerous properties which we believe are beneficial to high temperature strength and, accordingly, we will continue to study how to produce the elongated grain structure without concurrent loss due to melting.

For the balance of compositions in this grouping, aligned grain structures were obtained repeatedly. The criteria for abnormal grain growth which best fit this general class were that second phase dissolution take place at a temperature below that of incipient melting, but sufficiently high and at a rate so that, as pinning of equiaxed boundaries was eliminated, rapid grain boundary annihilation could take place.

### **DS Eutectic Types (RSR 97, 99, 100, 101, 102)**

We were unable to develop coarse grain structures in any of these alloys for reasons which we believe are similar to those of RSR 90, i.e., stable, somewhat coarse second phase precipitates which persisted beyond incipient melting. Further studies with these alloys will take place only if information received from work with the remaining compositions suggests renewing the effort.

### **Ni-Al-Mo Ternaries (RSR 103, 104, 105, 123)**

This entire group of alloys responded well to abnormal grain growth, however, the controlling factor is thought to be somewhat more complex in this series than in the conventional superalloy types. Our microstructural studies, and also those being conducted at the University of Florida on the same alloys, have shown that the rapid solidification caused the compositions to solidify to nonequilibrium phases of the type  $\text{Ni}_3(\text{Al}, \text{Mo})$ ,  $\text{Ni}_3\text{Mo}$ , and  $\text{NiAlMo}$ . Equilibrium states that  $\text{Ni}_3\text{Al}$ ,  $\text{NiMo}$  and  $\text{Mo}$  should exist. The two intermetallics in the RSR powders appeared stable to about  $0.9 T_m$ , at which time one or both underwent reactions to produce a finely dispersed Mo phase. Concurrent with this (or coincidentally), abnormal growth took place. As will be noted in the section on mechanical property testing, these reactions are of great interest and, therefore, extensive work toward better understanding of the nature and kinetics of these reactions is in progress.

### **High Gamma Prime Types (RSR 110, 111, 112, 113, 116, 117, 119)**

Only RSR 111, a 3.5% Hf, 0.17% C modification to a simple NiCrAl system, failed to respond to abnormal grain growth. The incipient melt temperature for this alloy was lowest, 2335°F (1279°C), of the class. For the other alloys, growth was achieved at temperatures typically

near 2400°F (1315°C). Failure of this particular alloy to respond is believed to be gross melting prior to achieving conditions favorable for the rapid grain growth. The remaining compositions behaved in a manner similar to that observed with the conventional types.

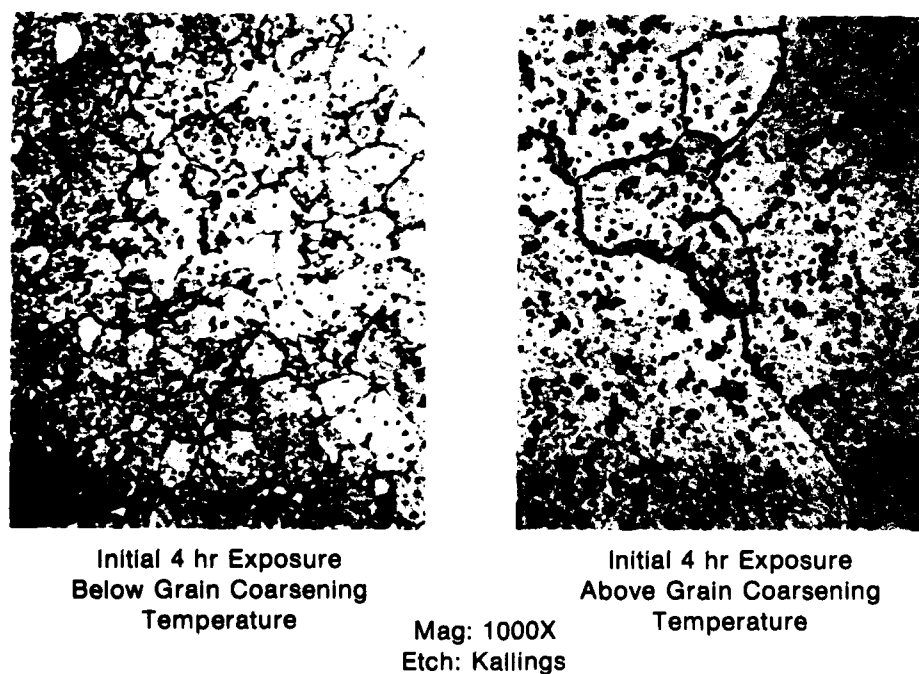
Several observations are worth noting here relative to the general nature of the aligned structures. First, once aligned, abnormal growth was initiated, it was uncommon to observe start/stop type activity. Secondly, those grains which started remained prevalent and continuous for the entire length of the bar undergoing zone annealing. Typical, also, were convoluted grain boundaries which did not present large planar areas nor did they present abrupt changes in direction when viewed on a micro scale. Finally, X-ray diffraction analyses of samples to date showed that the grain orientation was consistently (110).

### THERMAL STABILITY

The three alloy types which responded to abnormal grain growth were further subjected to thermal exposure at 1600°F (871°C) in order to determine whether instabilities would occur at intermediate temperature. Testing was carried out with sections of bars previously subjected to a gradient heat treat in which the temperature was varied from about 0.7  $T_m$  to essentially  $T_m$ . A 300-hr exposure was used for evaluating microstructural changes.

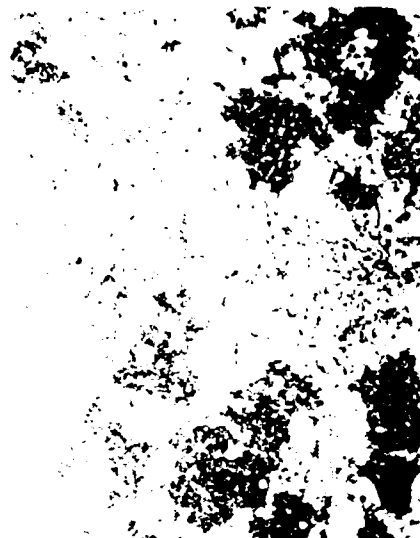
Results with RSR alloys 121 (conventional), 104 (Ni-Al-Mo ternary), and 116 (high  $\gamma'$ ) typify those for the entire series of compositions and are shown in Figures 1 through 3. In general, gradual coalescence of the  $\gamma'$  phase was the only observed difference, regardless of what prior solutioning and reprecipitation might have taken place during the gradient heat treat.

Degenerate reactions such as those leading to phase or grain boundary alteration were not detected. It is presumed that some carbide precipitation took place within the grain boundary regions for those alloys possessing the low temperature carbide forming elements, but not under conditions suggesting an instability of the type we were investigating.

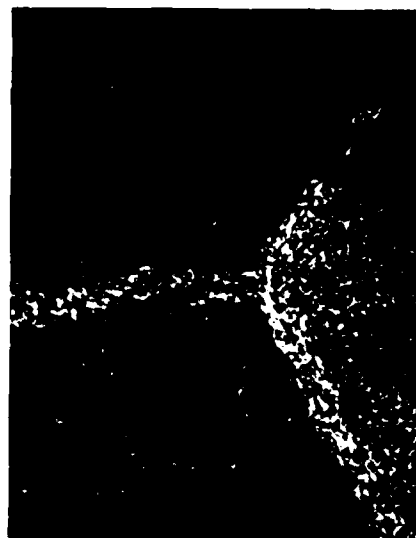


FD 127289

Figure 1. Thermal Stability of RSR 121 After 300 hr at 1600°F (871°C)



Initial 4 hr Exposure  
Below Grain Coarsening  
Temperature

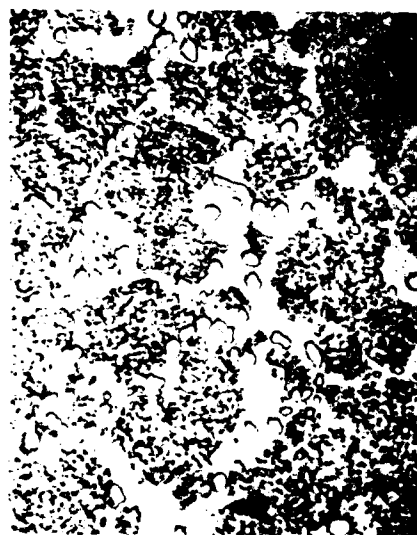


Initial 4 hr Exposure  
Above Grain Coarsening  
Temperature

Mag: 1000X  
Etch: Kallings

FD 127267

*Figure 2. Thermal Stability of RSR 104 After 300 hr at 1600°F (871°C)*



Initial 4 hr Exposure  
Below Grain Coarsening  
Temperature



Initial 4 hr Exposure  
Above Grain Coarsening  
Temperature

Mag: 1000X  
Etch: Kallings

FD 127268

*Figure 3. Thermal Stability of RSR 116 After 300 hr at 1600°F (871°C)*

## TEST RESULTS WITH ALIGNED GRAIN STRUCTURES

Thirteen of the fourteen alloys which responded effectively to zone annealing were tested in creep-rupture during this period. Subsequent to zone annealing and prior to test, the conventional and high  $\gamma$  type alloys were resolutioned and then given a coating simulation and age cycle of the type previously described. The Ni-Al-Mo ternaries were given only a resolution cycle. The temperatures used for solutioning are listed in Table 3. All heat treat cycles were completed by air cooling.

TABLE 3. SOLUTIONING TEMPERATURES  
USED TO HEAT TREAT EX-  
PERIMENTAL ALLOYS

Alloy	Temperature	
	°F	(°C)
110	2420	(1327)
112	2360	(1293)
113	2360	(1293)
116	2420	(1327)
117	2390	(1310)
119	2320	(1271)
108	2275	(1246)
121	2220	(1215)
122	2220	(1215)
124	2220	(1215)
103	2400	(1315)
104	2400	(1315)
123	2400	(1315)

Initially, the testing was started at 1900°F (1038°C) in a manner similar to that attempted with the equiaxed test bars, i.e., relatively low stress so that this same level could be repeated effectively at higher temperatures. Subsequently, the temperatures and stresses were varied to provide the information which we thought would be most relevant for this first set of test data.

All testing was done in air. Stress levels at the higher temperatures were appropriately corrected to account for density difference from the base alloy MAR M200. The results are listed in Table 4 and are grouped according to alloy category.

Although the data is very limited, all results were highly encouraging with respect to meeting program goals for creep resistance and creep-rupture strength. Within the conventional alloy group, little difference was evident for the various compositions in creep resistance or life in the tests where the duration was typically short. However, in the longer-time testing it appeared that the alloys with the higher interstitial element concentrations led to longer-rupture lives and better creep/resistance.

The Ni-Al-Mo ternaries, especially the alloy RSR 104, displayed excellent properties in terms of creep resistance and creep-rupture lives. The data obtained with RSR 104, in fact, meets the program objectives with respect to strength requirements at 1900°F (1038°C). For each of the alloy compositions in this group, strengthening appeared to be the result of a highly effective dispersion of Mo, occurring both as  $\text{Ni}_3(\text{Al}, \text{Mo})$  and as  $\alpha$  Mo. The microstructure of RSR 104 alloy, after zone annealing and as evidenced by transmission electron microscopy, is shown in Figure 4.

The structure consists of about 1  $\mu\text{m}$  cells of  $\gamma$ , with a complex dispersion of phases in the cell walls. Our identification studies to date indicate that at least one of the species within the cell wall is  $\alpha$  Mo, dispersed as a lath like precipitate on the order of 250 Å thick and 1 to 3000 Å long.



TABLE 4. CREEP-RUPTURE RESULTS OF RSR ALLOYS HAVING ALIGNED GRAIN STRUCTURES

ID	Temperature		Stress		1.0% hrs	Life hrs	El %	Minimum Creep Rate hr <sup>-1</sup> × 10 <sup>-3</sup>
	°F	(°C)	ksi	(MPa)				
57 <sup>1</sup>	1400	760	95.0	(65.5)	163.0	179.6	9.1	
57 <sup>1</sup>	1400	760	95.0	(65.5)	37.5	45.4	10.3	
57 <sup>1</sup>	1800	982	31.5	(217.2)	41.8	54.5	15.1	
57 <sup>1</sup>	1800	982	31.5	(217.2)	24.5	67.9	12.9	
58 <sup>1</sup>	1800	982	31.5	(217.2)	42.6	53.5	10.8	
60 <sup>1</sup>	1800	982	31.5	(217.2)	15.6	56.8	11.4	
60 <sup>1</sup>	1800	982	25.0	(172.4)	82.7	321.9	21.6	
61 <sup>1</sup>	1900	1038	20.0	(137.9)	28.6	52.0	N/R	
108	1900	1038	15.0	(103.4)	39.0	78.5	7.6	18
108	1900	1038	15.0	(103.4)	54.6	147.1	12.4	11
108	2000	1093	15.0	(103.4)	12.0	15.1	7.2	
121	1400	760	90.0	(620.5)	14.2	68.2	13.2	
121	1800	982	30.5	(210.3)	32.4	44.4	12.9	20
121	1900	1038	14.4	(99.3)	104.8	218.8	8.5	5
121	2000	1093	14.4	(99.3)	9.6	13.7	15.5	
122	1800	982	30.5	(210.3)	24.5	47.3	22.9	29
122	1900	1038	14.4	(99.3)	157.3	219.9	8.4	3
124	1900	1038	15.0	(103.4)	189.0	241.7	11.1	3
124	2000	1093	15.0	(103.4)	13.6	16.6	5.6	
103	1400	760	90.0	(620.5)	80.6	110.6	4.7	7
103 <sup>2</sup>	1400	760	90.0	(620.5)	16.1	22.8	2.3	40
103 <sup>2</sup>	1800	982	30.0	(206.8)	9.9	10.3	4.1	
103	1800	982	30.0	(206.8)	17.6	73.7	16.4	40
103	1900	1038	21.5	(148.2)	35.5	44.1	N/R	16
103	2000	1093	14.2	(97.9)	222.0	288.2	2.6	3
104	1400	760	100.0	(689.5)	23.3	25.6	10.9	
104	1400	760	90.0	(620.5)	205.4	(Still on Test)		
104	1800	982	30.0	(206.8)	132.0	221.4	5.6	4
104	1800	982	30.0	(206.8)	116.0	182.8	4.3	14
104	1900	1038	30.0	(206.8)	42.6	59.1	4.0	5
104	1900	1038	30.0	(206.8)	28.3	33.9	2.9	22
104	1900	1038	14.2	(97.9)	660.2	908.2	3.4	1
104	2000	1093	14.2	(97.9)	79.6	493.3	3.6	7
123	1900	1038	14.2	(97.9)	12.2	33.9	7.4	68
110	1900	1038	14.2	(97.9)	17.9	42.6	10.3	31
112	1900	1038	13.5	(93.1)	15.5	68.8	25.5	72
113	1900	1038	13.5	(93.1)	32.3	68.4	14.0	13
113	1900	1038	13.5	(93.1)	25.6	99.8	20.1	19
116	1900	1038	14.2	(97.9)	114.0	149.9	9.4	3
116 <sup>3</sup>	1900	1038	14.2	(97.7)	52.0	(Discontinued)		9
116	2000	1093	14.2	(97.9)	8.3	14.8	4.4	
117	1900	1038	14.2	(97.9)	22.6	63.2	13.2	22
117	2000	1093	14.2	(97.9)	3.4	14.4	12.6	
119	1900	1038	13.5	(93.1)	33.5	111.2	21.5	13
119	1900	1038	13.5	(93.1)	33.9	95.7	19.3	34

<sup>1</sup>Alloy and heat treat same as RSR 108

<sup>2</sup>No solution after zone annealing

<sup>3</sup>Possible heat treat error

N/R -- Not recorded

The high  $\gamma$  alloy series also displayed excellent properties, especially in light of the simplicity of the alloy compositions. There did not appear to be any large deviations in properties as a result of our composition changes, except perhaps for alloy 116, which showed significantly better creep resistance at 1900°F (1038°C) than the others. However, as with the other alloy groups, with testing as limited as what we have to date, it is difficult to generalize or speculate as to the value of the individual alloy additions.

Figure 5 shows 1900°F (1038°C) creep curves which we believe typify the behavior of the individual alloy categories. In each case, it was evident that all three stages of creep (primary, secondary, and tertiary) occurred, with primary creep most pronounced in the conventional alloy system. Tertiary creep was more evident with the conventional and high  $\gamma$  type alloys but for all three it accounted for an equal portion of life (approximately 33% of total). No noticeable deviations in second stage creep rates were detected for any of the alloys tested.

Figures 6 and 7 are parametric displays of some of the test data for times to 1% creep and rupture life. They are included for the readers benefit to enable comparison of properties with those of other alloys.

Figure 8 shows the fracture characteristics of the experimental test bars. The equiaxed bar obviously reflects intergranular fracture with little, if any, indication of reduction in gage cross-sectional area. The aligned grain structures show exactly the opposite.

The 2 lower photos in the figure show how the grain boundaries in the aligned structures (which were described previously as convoluted) might be contributing to overall strength of the alloy. The RSR 104 alloy showed grain boundary fissuring somewhat more extensively than we had expected and certainly suggested that the boundaries played a significant role in the process leading to failure. Also, for the alloy 116, the test bar used in the 1900°F (1038°C), 14.2 ksi (97.9 MPa) was actually a single crystal, and the data from this test was noticeably better than others in the series. Viewed in conjunction with the observations that the higher interstitial concentrations in the conventional alloy series seemed to promote creep resistance, then it is reasonable to believe that the boundary contribution to creep of these structures is more than incidental and should be treated accordingly.

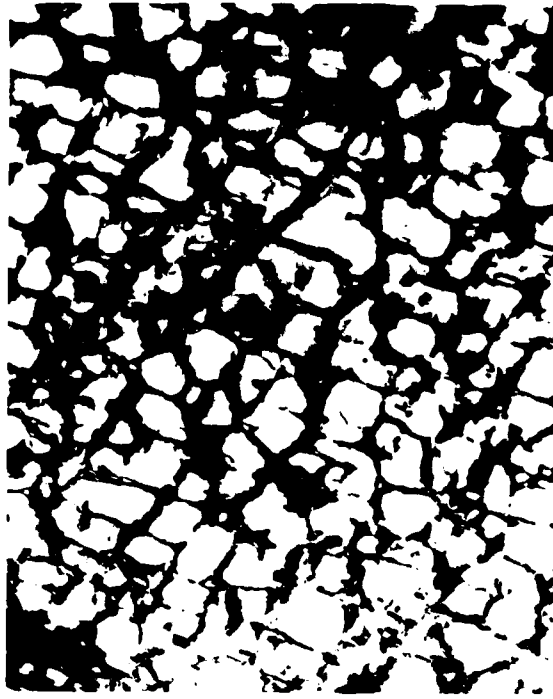
Even though the data were scarce for the various forms, we did attempt to calculate activation energy for matrix creep of MAR M200 alloy in order that we could compare the value obtained to those of MAR M200 castings. The results are listed in Table 5 and, in our opinion, reflect values one would expect. The actual differences appear to be within experimental error, and the trend indicated by the data, i.e., higher  $Q$  in the forgings, is thought to be coincidental.

TABLE 5. ACTIVATION ENERGY  
FOR MATRIX CREEP IN  
MAR M200 ALLOY

(1800 to 1900°F Test Range)  
(982 to 1038°C)

Alloy Form	$Q$
	Kcal/m
Equiaxed Casting	121
Directionally Solidified Casting	127
Equiaxed Forging	131
Directional Grain Forging	137

The microstructures of RSR alloys 121, 116, and 104 after creep-rupture testing are shown in Figures 9 through 12 and describe the changes in structure as a result of both the time at temperature and the influence of stress. RSR 121, the conventional superalloy type, underwent fairly rapid coalescence of the  $\gamma$  phase at 1800°F (982°C), with the effect of stress very evident on the nature of growth. At 1900°F (1038°C), dissolution and reprecipitation was extensive. RSR alloy 116, the high  $\gamma$  type, showed similar features to that of the 121 alloy but on a much-reduced scale relative to rates of coalescence and dissolution. RSR alloy 104, on the other hand, showed only minor changes in base alloy microstructure relative to phase growth, no indications of phase dissolution, and no indication that stress changed or contributed to phase reaction rates. These observations are as one would expect in light of the test data and alloy composition.

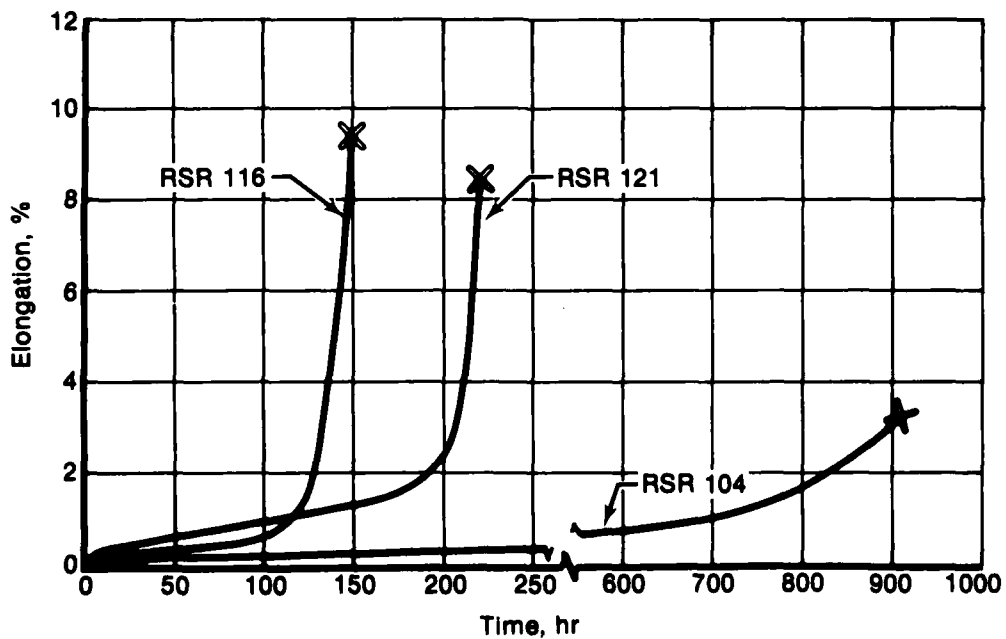


Mag: 35000X

Bright Field Image

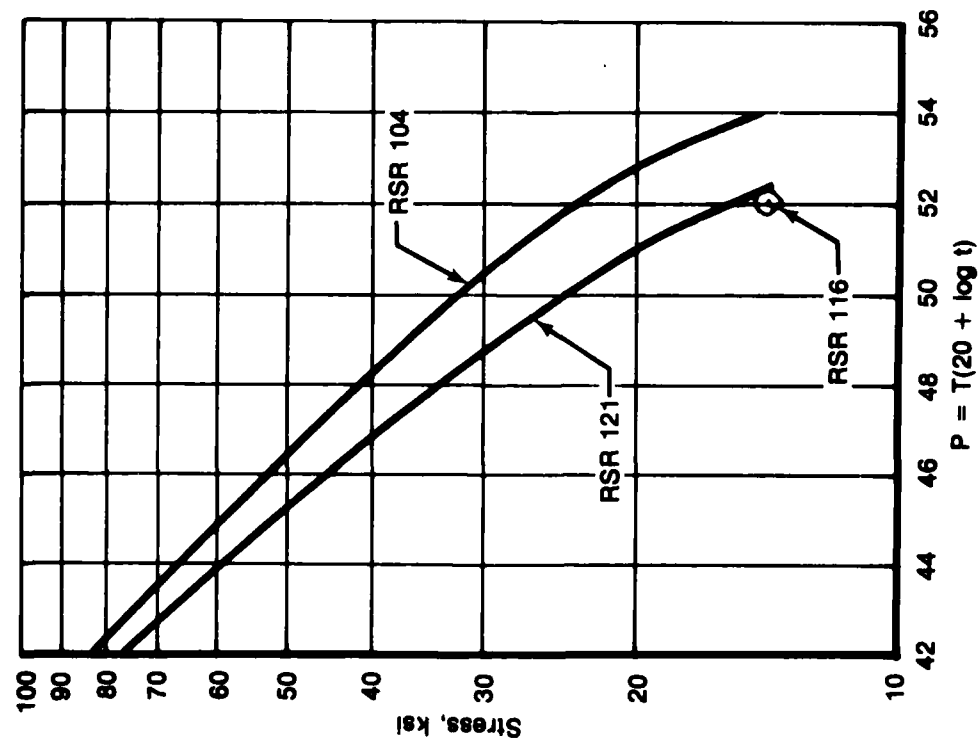
FD 127266

Figure 4. Transmission Photomicrograph Showing the Structure of RSR 104 After Zone Annealing



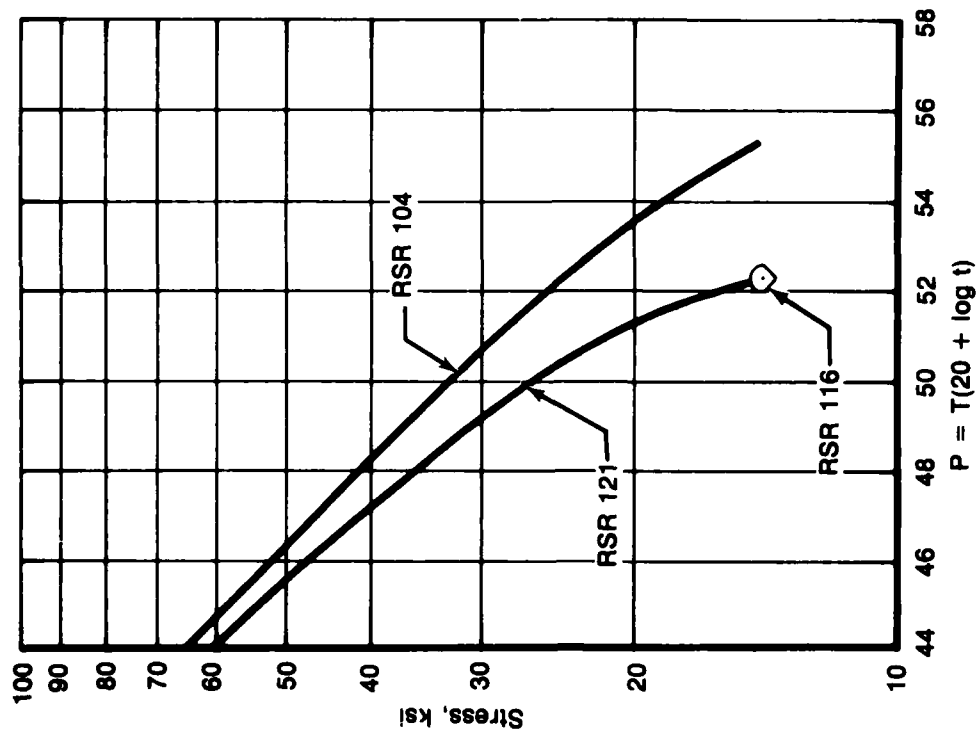
FD 127264

Figure 5. Typical Creep Deformation of Experimental Alloys at 1900°F (1038°C) and 14.2 ksi (97.9 MPa)



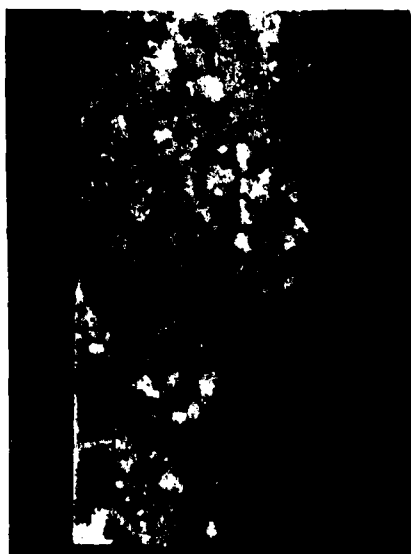
FD 127-263

Figure 6. Creep Resistance of Experimental Alloys (Time to 1% Elongation)



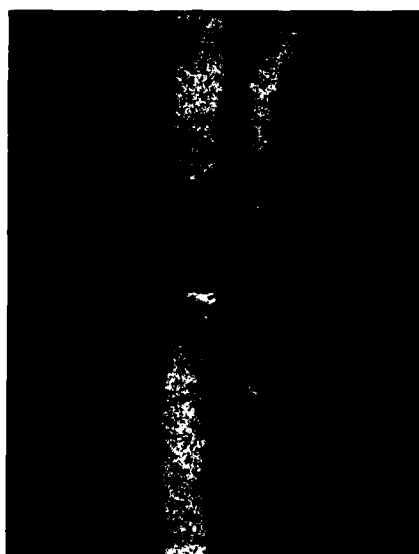
FD 127-262

Figure 7. Stress-Rupture Life of Experimental Superalloys



Mag: 10X

Equiaxed Grain  
RSR 122



Mag: 10X

Directional Grain  
RSR 122



Mag: 25X

Directional Grain  
RSR 104

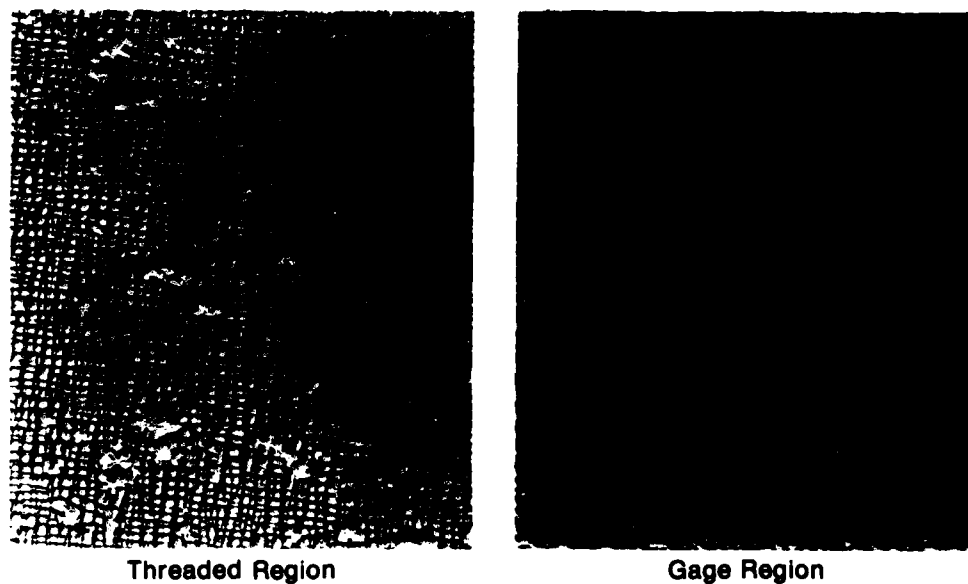


Mag: 25X

Single Crystal  
RSR 116

FD 12726

*Figure 8. Typical Failure Characteristics of Experimental Superalloys*



Threaded Region

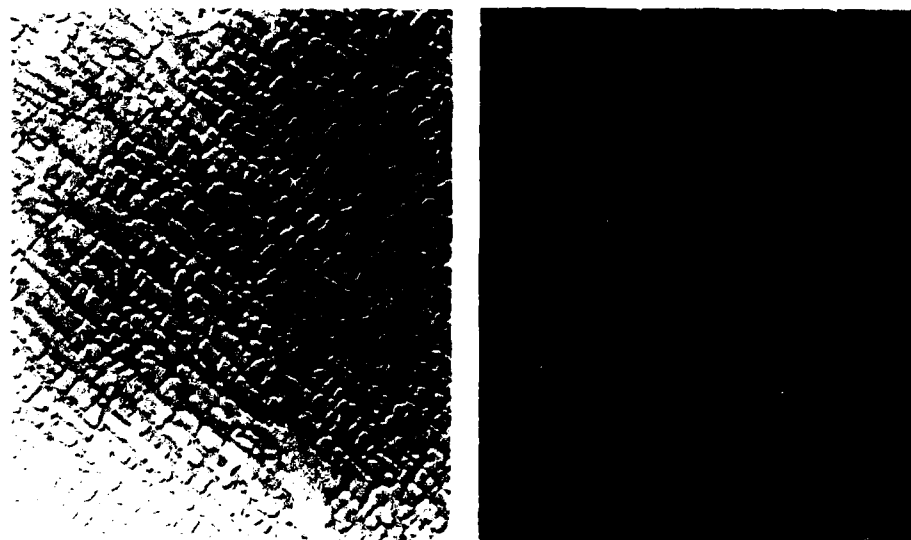
Gage Region

Mag: 3000X

Etch:  $\text{H}_2\text{SO}_4$ ,  $\text{HNO}_3$ ,  $\text{H}_3\text{PO}_4$ , electrolytic

FD 127271

*Figure 9. Microstructure of RSR 121 After Creep-Rupture Testing at 1800°F (982°C) and 30.5 ksi (210.3 MPa), Failure Time = 44 hr*



Threaded Region

Gage Region

Mag: 3000X

Etch:  $\text{H}_2\text{SO}_4$ ,  $\text{HNO}_3$ ,  $\text{H}_3\text{PO}_4$ , electrolytic

FD 127272

*Figure 10. Microstructure of RSR 121 After Creep-Rupture Testing at 1900°F (1038°C) and 14.4 ksi (99.3 MPa), Failure Time = 219 hr*



Threaded Region



Gage Region

Mag: 3000X

Etch:  $\text{H}_2\text{SO}_4$ ,  $\text{HNO}_3$ ,  $\text{H}_3\text{PO}_4$ , electrolytic

FD 127271

*Figure 11. Microstructure of RSR 116 After Creep-Rupture Testing at 1900°F (1038°C) and 14.4 ksi (99.3 MPa), Failure Time = 149 hr*



Threaded Region



Gage Region

Mag: 3000X

Etch:  $\text{H}_2\text{SO}_4$ ,  $\text{HNO}_3$ ,  $\text{H}_3\text{PO}_4$ , electrolytic

FD 127270

*Figure 12. Microstructure of RSR 104 After Creep-Rupture Testing at 1900°F (1038°C) and 30 ksi (206.8 MPa), Failure Time = 34 hr*

### SECTION III

#### ON-GOING STUDY

On the basis of test data obtained during this report period, we have expanded our alloy development activities in 3 categories. The first is to investigate conventional type superalloys relative to producing much higher  $\gamma'$  concentrations of the type observed in the 110 to 118 series but without inducing instability. The second is to investigate how grain boundary contributions might be controlled in the high  $\gamma'$  and Ni-Al-Mo type. The third is to study in more detail composition effects leading to the observed strengthening characteristics in the Ni-Al-Mo series. The results of this expansion, as well as additional test data from the alloys already described, will be reported in subsequent reports.



4

**END**

**FILMED**

**9-83**

**DTIC**